

## Supporting Information

### **Crucial Roles of Triazinic-N=O and C=O Groups in Photocatalytic Water Splitting on Graphitic Carbon Nitride**

Huizhong Ma<sup>1,2</sup>, Xiao Zhang<sup>1,2</sup>, Fan Jin<sup>1</sup>, He Zhou<sup>1</sup>, Jie Zhang<sup>1</sup> and Yuchen Ma<sup>1,3</sup>

<sup>1</sup>School of Chemistry and Chemical Engineering, Shandong University, Jinan, China

<sup>2</sup>Authors contributed equally

<sup>3</sup>E-mail: myc@sdu.edu.cn

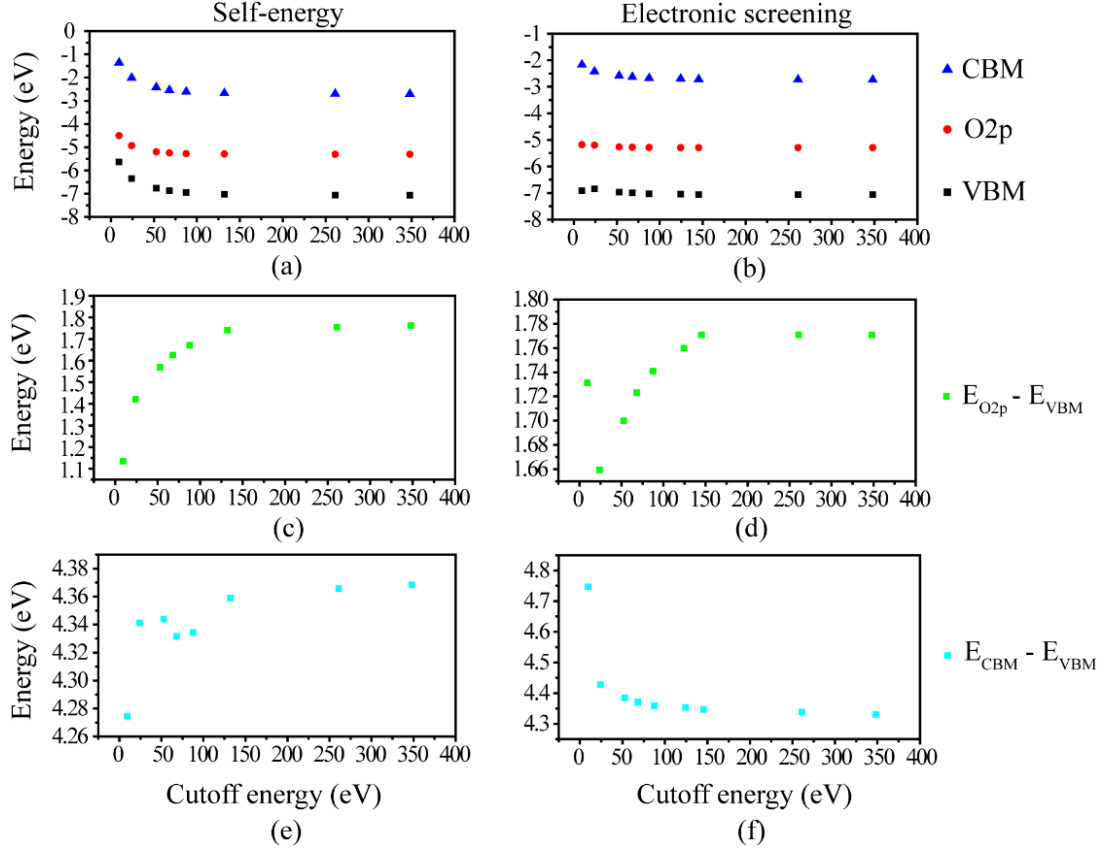


Fig. S1 Evolution of orbital (CBM, VBM, the highest occupied O 2p) energies [(a) and (b)] and their gaps [(c), (d), (e) and (f)] at  $\Gamma$  point for the structure OH&N-H (see the structure II in Fig. 2b of the main context) with the cutoff energy applied in the band summation over unoccupied orbitals for the evaluation of self-energy [(a), (c) and (e)] and electronic screening [(b), (d) and (f)] in GW. Value of the cutoff energy is relative to CBM. When testing the convergence of self-energy as illustrated in (a), (c) and (e), cutoff energy in the evaluation of electronic screening is set to 88 eV. When testing the convergence of electronic screening as illustrated in (b), (d) and (f), cutoff energy in the evaluation of self-energy is set to 132 eV. We finally choose 260 eV and 145 eV as the cutoff energies respectively for the self-energy and electronic screening in the routine GW calculations of this work. Orbital energies and their gaps could converge to 0.1 eV under these settings.

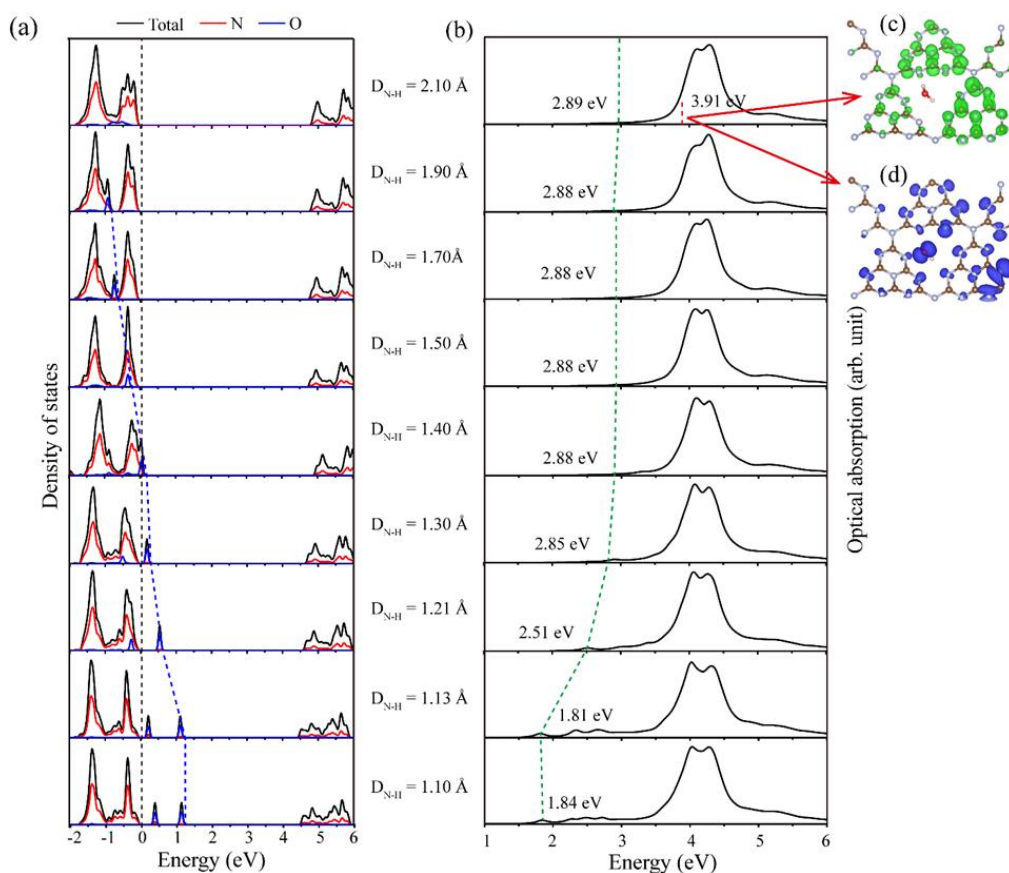


Fig. S2 Evolution of total and projected DOSs computed by GW (a) and optical absorption spectra computed by BSE (b) with the H transfer from H<sub>2</sub>O to a triazinic N.  $D_{N-H}$  is the distance between this H and the triazinic N as illustrated in Fig. 2b of the main context. In this process, coordinates of the remaining OH in H<sub>2</sub>O were fully relaxed, while those of all the other atoms were fixed at the optimized values before H transfer, just as stated in the main context. In (a), VBM is set to energy zero for each system. DOSs presented here are the sum of spin-up and spin-down channels. Evolution of the highest occupied projected DOS peaks onto the O atom is highlighted by a blue dashed line. In (b), evolution of the lowest excited states is highlighted by a green dashed line. (c) and (d) show spatial distributions of the photoelectron (green isosurfaces) and hole (blue isosurfaces) for the excited state at 3.91 eV when  $D_{N-H}$  equals 2.10 Å. In this excited state, charge-transfer transition with the hole localized on the O atom of H<sub>2</sub>O begins to emerge. Brown, light blue, red and pink balls in (c) and (d) represent C, N, O and H atoms respectively.

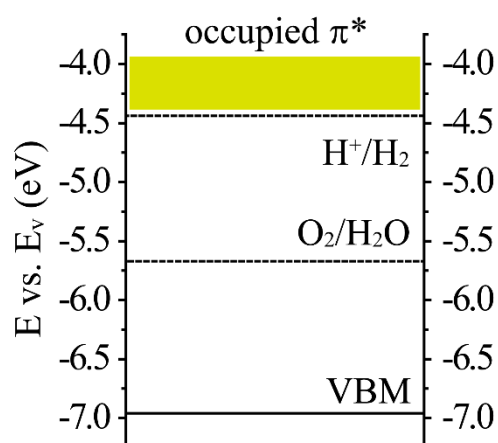


Fig. S3 Comparison between the energy levels (yellow bar) of electrons occupying the  $\pi^*$  orbitals of N-OH&N-H (see Fig. 3 of the main context for its geometry) and the redox potentials for water splitting.  $E_v$  is the vacuum level. Position of VBM is set according to the ionization energy of g-C<sub>3</sub>N<sub>4</sub> as measured in experiments [e.g. Science 347, 970 (2015)]. Energy range of the yellow bar with respect to VBM is set to the same as energy range of the occupied DOS peaks within the band gap with respect to VBM as shown in Fig. 3a for N-OH&N-H.

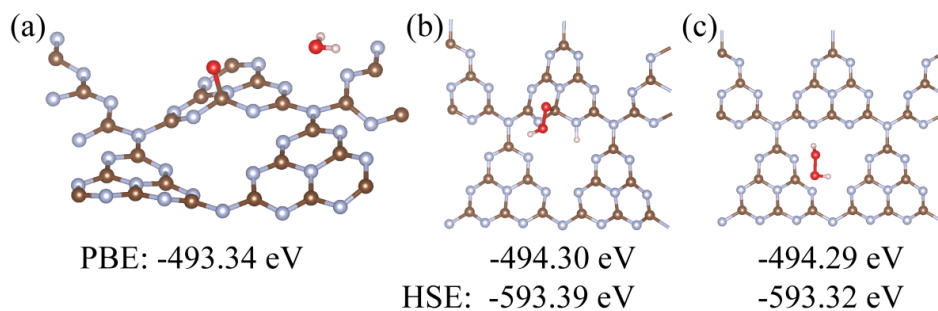


Fig. S4 Geometries and potential energies of the reactant (a) and products (b, c) for the splitting reaction of a H<sub>2</sub>O molecule at C=O in the ground state. (a) A H<sub>2</sub>O molecule lies far away from C=O and g-C<sub>3</sub>N<sub>4</sub>. (b) H<sub>2</sub>O is split into a C-OOH&N-H pair. (c) A H<sub>2</sub>O<sub>2</sub> molecule is formed from C-OOH&N-H. Geometries were optimized by DFT-PBE. Potential energies computed by DFT-PBE and DFT-HSE based on the DFT-PBE geometries are both given for comparison.

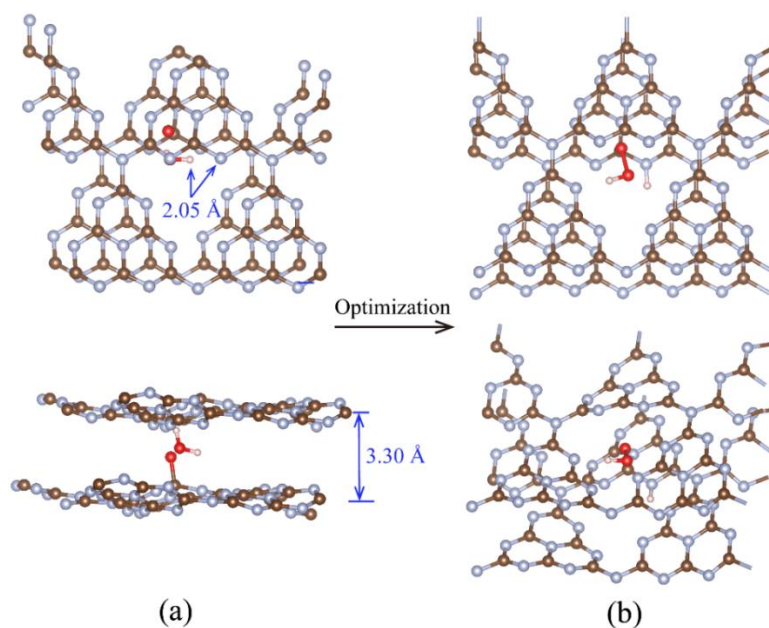


Fig. S5 Spontaneous splitting of the second H<sub>2</sub>O molecule at C=O in the ground state in the presence of another g-C<sub>3</sub>N<sub>4</sub> layer. The average interlayer distance between the two g-C<sub>3</sub>N<sub>4</sub> layers was set to 3.30 Å. Putting a H<sub>2</sub>O molecule near C=O with the distance between one H in H<sub>2</sub>O and the triazinic N with which this H would bond being 2.05 Å (a), this H<sub>2</sub>O would split into a C-OOH&N-H complex (b) after geometry optimization in the ground state. Top panels and bottom panels in (a) and (b) show the top and the side views of the system respectively.

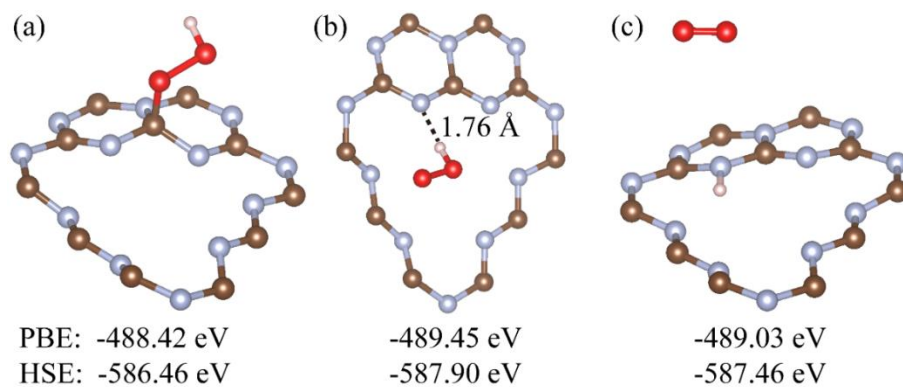


Fig. S6 Relative energies between C-OOH (a), HO<sub>2</sub> (b) and O<sub>2</sub>&N-H (c). Geometries were optimized by DFT-PBE. Potential energies computed by DFT-PBE and DFT-HSE based on the DFT-PBE geometries are both given for comparison.

Table S1 Potential energies of an isolated H, HO<sub>2</sub> and H<sub>2</sub>O<sub>2</sub> computed by DFT-PBE using the VASP code.

	PBE
H	-1.12 eV
HO <sub>2</sub>	-13.25 eV
H <sub>2</sub> O <sub>2</sub>	-18.15 eV

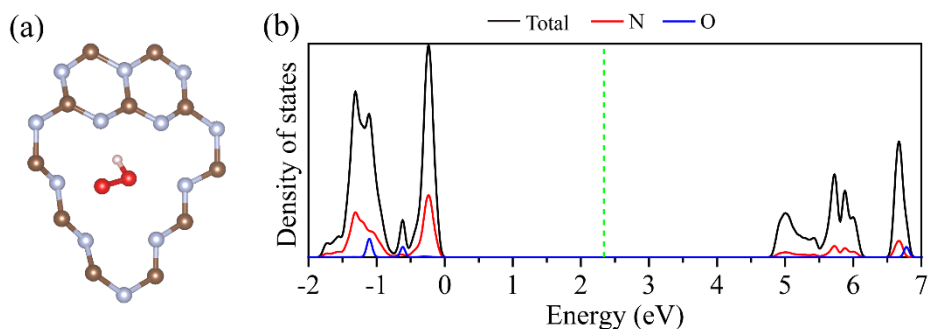


Fig. S7 Geometry (a), total and projected DOSs computed by GW (b) for a HO<sub>2</sub> molecule adsorbed onto g-C<sub>3</sub>N<sub>4</sub>. VBM is set to energy zero. The green dashed line marks position of the Fermi level which is defined here as the middle between the highest occupied electronic level and CBM.

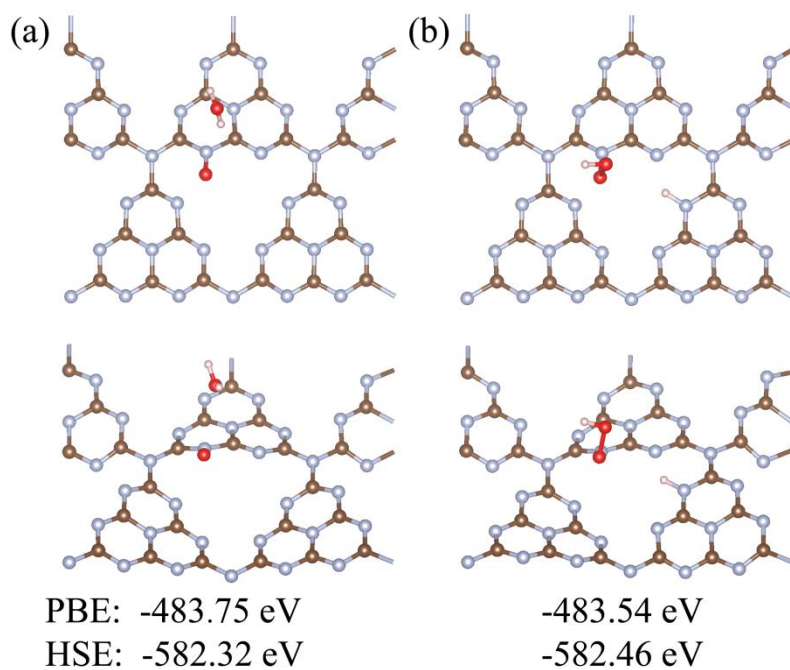


Fig. S8 (a) A H<sub>2</sub>O molecule is placed far away from a N=O<sup>2+</sup> in the g-C<sub>3</sub>N<sub>4</sub> doped by two holes. (b) A N-OOH<sup>2+</sup> & N-H complex in the g-C<sub>3</sub>N<sub>4</sub> doped by two holes. Top panels and bottom panels in (a) and (b) show different views of the systems respectively. Geometries were optimized by DFT-PBE. Potential energies computed by DFT-PBE and DFT-HSE based on the DFT-PBE geometries are both given for comparison.

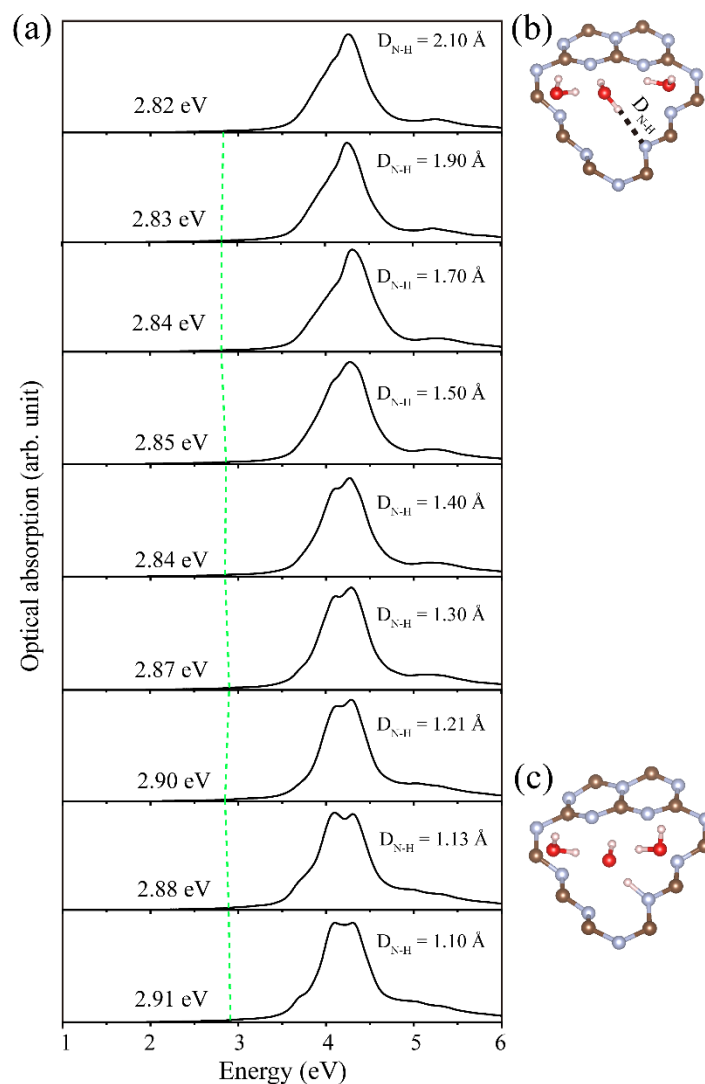


Fig. S9 (a) Evolution of optical absorption spectra computed by BSE with the H transfer from H<sub>2</sub>O to a triazinic N for the complex OH&N-H&2H<sub>2</sub>O<sup>a</sup>.  $D_{N-H}$  is the distance between this H and triazinic N as illustrated in (b). For each  $D_{N-H}$ , coordinates of atoms in the split H<sub>2</sub>O and g-C<sub>3</sub>N<sub>4</sub> were fixed to the same values as those of the corresponding complex studied in Fig. S2, while coordinates of the two additional H<sub>2</sub>O molecules were fully relaxed. Evolution of the lowest excited states is highlighted by the green dashed line. (b) [(c)] Geometry when  $D_{N-H}$  equals 2.10 Å [1.13 Å]. The lowest excited state is a  $n\pi^*/\pi\pi^*$  transition for each  $D_{N-H}$ .



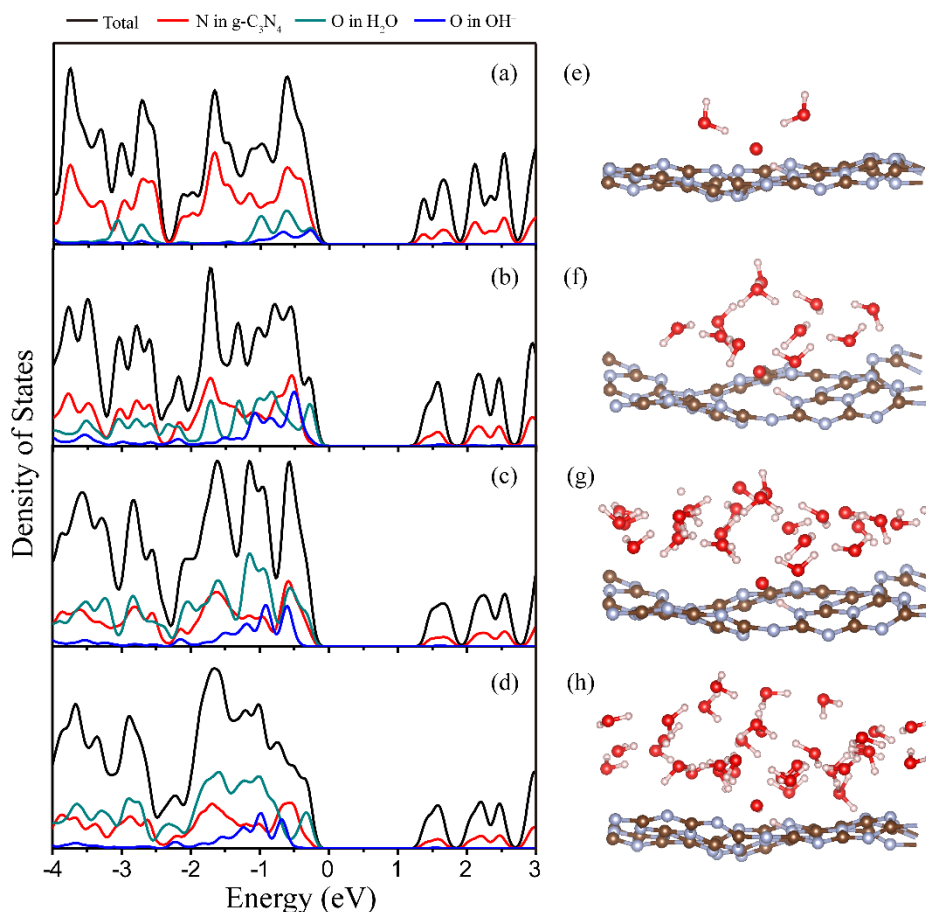


Fig. S10 (a) Total and projected DOSs computed by DFT-PBE for the complex OH&N-H<sub>1.13</sub>&2H<sub>2</sub>O<sup>a</sup> whose geometry is shown in (e) and is also the same as that shown in the right panel of Fig. 6c of the main context. (b)/(c)/(d) Total and projected DOSs computed by DFT-PBE when 8/21/26 more water molecules were added into OH&N-H<sub>1.13</sub>&2H<sub>2</sub>O<sup>a</sup> to form a larger hydrogen bond network. Their relaxed geometries in the ground state are shown in (f), (g) and (h). More information can be got from the caption of Fig. 6 in the main context. VBM is set to energy zero for each system. Since GW calculations are extremely heavy for the big systems in (g) and (h), DFT DOSs are compared here instead. Although the absolute values of electronic levels are not predicted well by DFT, DFT may give reasonable prediction for the relative variation of electronic levels. From the DOSs, it can be seen that O 2p levels of the split H<sub>2</sub>O (the blue curve) downshift gradually with the increase of water molecules.

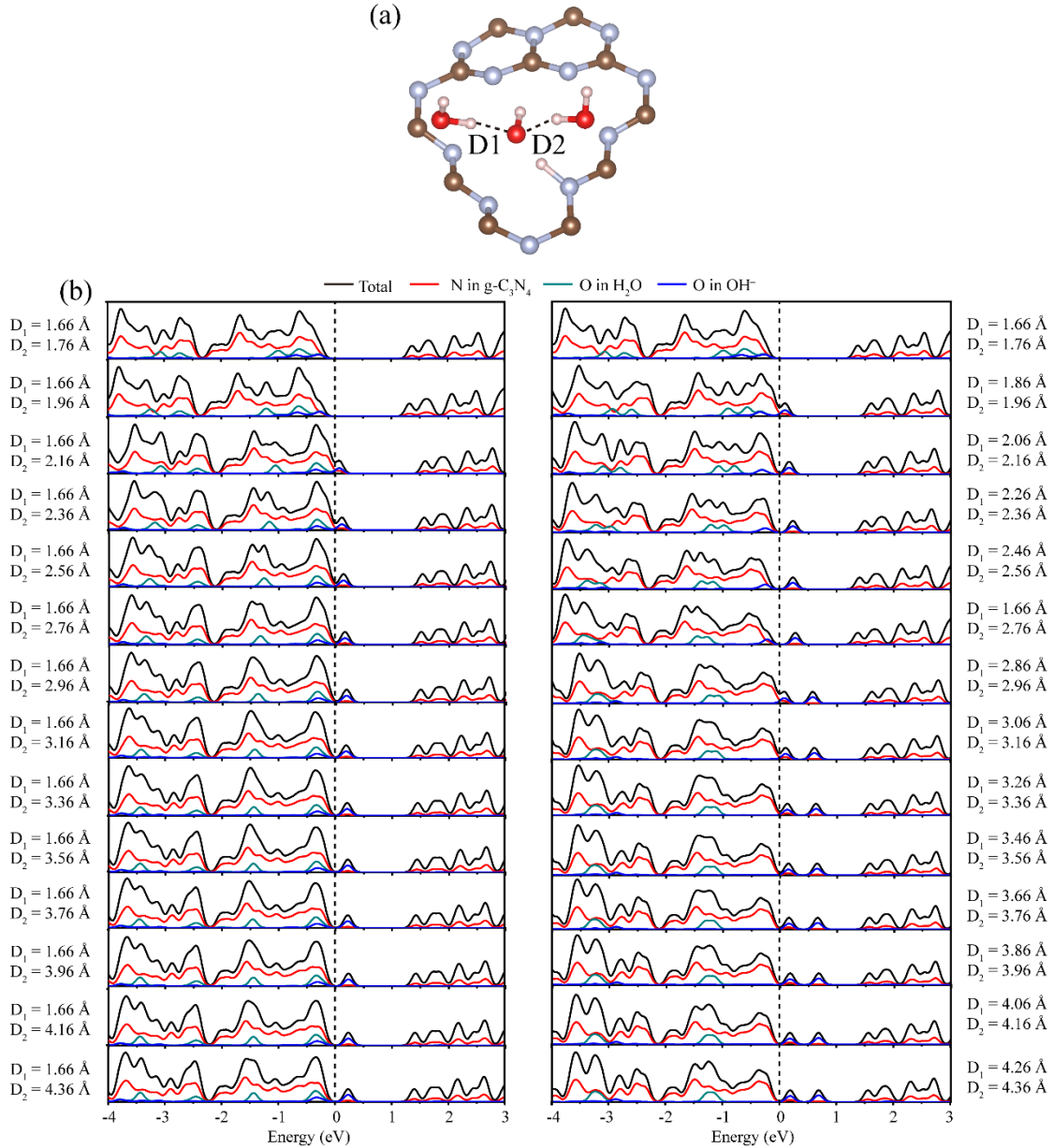


Fig. S11 (a) Geometry of the complex  $\text{OH}\&\text{N-H}_{1.13}\&2\text{H}_2\text{O}^a$ .  $D_1$  and  $D_2$  denote lengths of the two hydrogen bonds. (b) Evolution of total and projected DOSs computed by DFT-PBE with the variation of  $D_1$  and  $D_2$ . For each pair of  $D_1$  and  $D_2$ , coordinates of atoms in the split  $\text{H}_2\text{O}$  and  $\text{g-C}_3\text{N}_4$  were fixed to their initial values when  $D_1$  equals 1.66 Å and  $D_2$  equals 1.76 Å, while coordinates of atoms in the two additional  $\text{H}_2\text{O}$  molecules were fully relaxed. In the left panels,  $D_1$  is fixed at 1.66 Å, while  $D_2$  increases by 0.2 Å each time. In the right panels, both  $D_1$  and  $D_2$  increase by 0.2 Å each time. VBM is set to energy zero for each system.

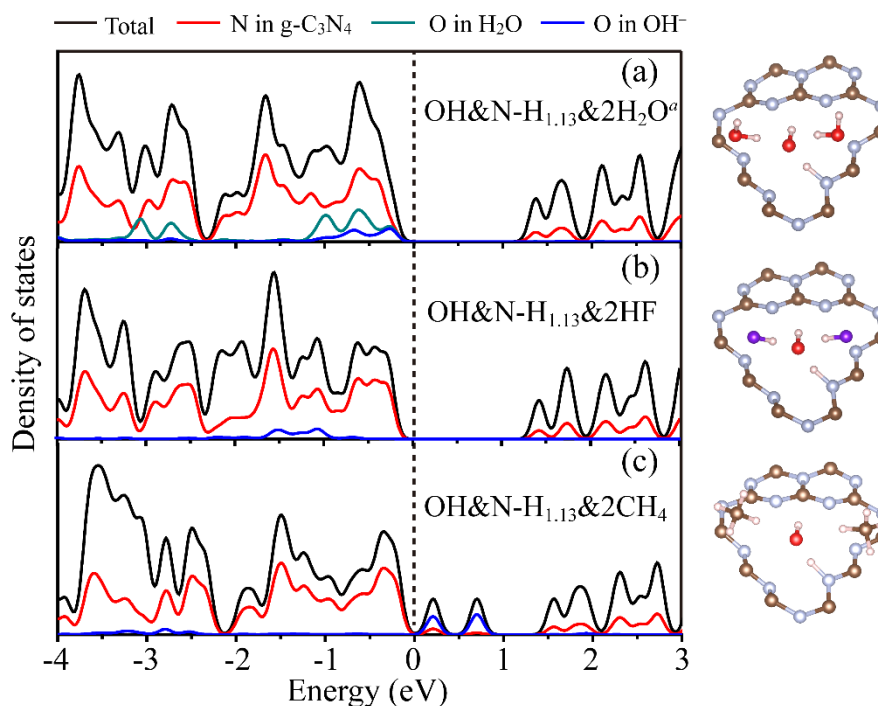


Fig. S12 Total and projected DOSs computed by DFT-PBE when two additional H<sub>2</sub>O molecules (a), two HF molecules (b) and two CH<sub>4</sub> molecules (c) were added respectively into the complex OH&N-H<sub>1.13</sub>. VBM is set to energy zero for each system. Right panels show the corresponding geometries. Each of these additional molecules form a hydrogen bond with OH. These DOSs demonstrate that with the increasing polarities of additional molecules, O 2p levels of OH downshift gradually. CH<sub>4</sub> is a nonpolar molecule. The highest O 2p level of OH&N-H<sub>1.13</sub>&2CH<sub>4</sub> is nearly 1 eV higher than that of OH&N-H<sub>1.13</sub>&2H<sub>2</sub>O<sup>a</sup>. Brown, light blue, red, violet and pink balls in the right panels represent C, N, O, F and H atoms respectively.



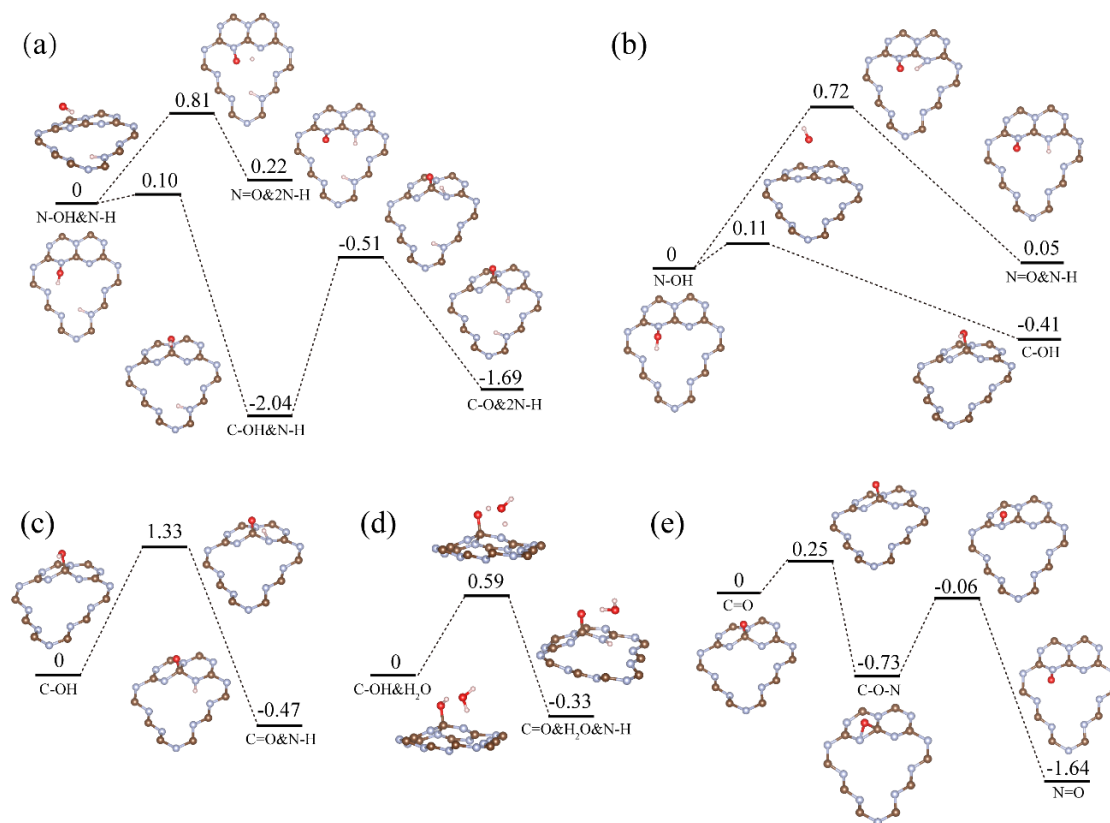


Fig. S14 The same as Fig. 4 except that the energies here were computed by DFT-HSE based on the geometries optimized by DFT-PBE. Comparison with Fig. 4 demonstrates that the conclusions based on DFT-PBE are reasonable and reliable.